The effect of subwafer dielectrics on plasma properties in plasma etching reactors

Robert J. Hoekstra and Mark J. Kushner
University of Illinois, Department of Electrical and Computer Engineering, 1406 West Green Street, Urbana, Illinois 61801

(Received 25 October 1994; accepted for publication 20 December 1994)

Nonplanar electrode topographies in plasma etching reactors are known to perturb plasma properties. In this article results from a computational study of plasma etching reactors having nonuniform dielectric structures *below* the wafer are presented. The system is an inductively coupled plasma reactor having a 13.56 MHz bias applied to the substrate. The model we have used is a hybrid simulation consisting of electromagnetics, electron Monte Carlo and fluid kinetics modules, and an off-line plasma chemistry Monte Carlo simulation. We found that the subwafer dielectric adds a series capacitance to the sheath and wafer resulting in voltage division of the applied potential between the sheath, wafer, and dielectric. This produces a smaller sheath potential and smaller sheath thickness above the dielectric. The ion energy distribution is therefore depressed in the vicinity of the dielectric. The effect is more severe at high plasma densities where the capacitance of the sheath is larger compared to the subwafer dielectric. © *1995 American Institute of Physics.*

I. INTRODUCTION

The surface topography of wafers, and the profile of mechanical structures in contact with the plasma, are known to affect the uniformity of the plasma and the quality of the product during the plasma etching of microelectronic devices.[1,2] The electric field enhancement which occurs at the edges of grooves, wafers, electrodes, wafer clamps, and other structures cause local perturbations in the plasma potential and subsequently in the electron impact source functions. The resulting perturbations in the ion flux (either in its magnitude or energy distribution) and radical flux can cause non-uniformities in etching characteristics. Typically, any discontinuity in permittivity caused by either geometry or material properties will, in a bounded system, perturb the plasma potential. Although these perturbations are generally undesirable, they have been capitalized to control of dust particle contamination of wafers. Dust particle traps can be created or controlled by strategic placement of structures which produce local extrema in the plasma potential or ion flux.[3]

If one broadens their view of the "electrical system" of the plasma to include the structural materials of the reactor, then it is reasonable to expect that discontinuities in permittivity below the wafer may also perturb plasma properties by changing the electrical boundary condition at the edge of the plasma. For example, dielectric structures below the wafer can act as capacitors which change the local impedance and, as a result, perturb the local current density. This phenomenon has been independently experimentally observed in the context of the control of dust particle traps.[4]

In this article we will computationally demonstrate the consequences of dielectrics located below the wafer on plasma properties in inductively coupled plasma (ICP) etching reactors having an rf bias on the substrate.[5–13] We find that the subwafer dielectrics modify the local impedance by adding a series capacitance to the sheath and wafer. If the capacitance of the dielectric is small, voltage division by the dielectric reduces the sheath voltage. This results in a reduction in the ion energy and displacement current, and possibly in the ion flux, to the wafer above the dielectric. The models we have used in this study will be briefly described in Sec. II. Our results are discussed in Sec. III, followed by our concluding remarks in Sec. IV.

II. DESCRIPTION OF THE MODELS

The computer models we have used in this study have been previously described,[14–16] and so will be only briefly discussed here. The two-dimensional simulation, called a hybrid plasma equipment model (HPEM), is composed of a series of modules which are iterated to a converged solution. The electromagnetics module (EM) generates inductively coupled electric and magnetic fields in the reactor. These fields are next used in the electron Monte Carlo simulation (EMCS) module. In the EMCS electron trajectories are followed for many rf cycles producing the electron energy distribution as a function of position and phase. These distributions are used to produce electron impact source functions which are transferred to the fluid kinetics simulation module (FKS). In the FKS, continuity and ion momentum equations are solved for all neutral and charged particle densities, and Poisson's equation is solved for the electric potential. The resulting plasma conductivity is passed to the EM. The species densities and time-dependent electrostatic potential are passed to the EMCS. The modules are iterated until cycle averaged plasma densities converge. Acceleration algorithms are used to speed the rate of convergence of the model.

At the end of the HPEM electron impact source functions and time-dependent electric fields are exported to the plasma chemistry Monte Carlo simulation (PCMCS).[14,15,17] The PCMCS launches pseudoparticles representing ions and

[a]Electronic mail: mjk@uiuc.edu

 0021-8979/95/77(8)/3668/6/$6.00 © 1995 American Institute of Physics

neutral species during the rf cycle from locations weighted by the electron impact source functions obtained from the HPEM. The trajectories of the pseudoparticles are followed in a time-dependent fashion using interpolated electric fields (position and phase). Surface reactions are represented by reactive sticking coefficients. Particle-mesh algorithms are used to represent ion-ion, ion-radical, and radical-radical collisions. In doing so, statistics on the densities of radicals and ions are collected during the flight of the pseudoparticles and transferred to the mesh. The pseudoparticles then collide with the mesh defined densities. A converged solution is obtained by iterating through many flights (or launchings) of pseudoparticles.

In an improvement to the previously described models, we have implemented a semianalytic sheath model in the HPEM and PCMCS to address conditions where the mesh spacing, Δx, exceeds the actual sheath thickness, λ_s, at boundaries. If the mesh is too coarse to resolve the sheath, the apparent sheath thickness is that of the mesh spacing adjacent to the wall. The sheath voltage is then dropped across the width of the numerical cell. For low pressures where the sheath is collisionless, the sheath voltage and other parameters are little affected by the artificially large sheath thickness. However, in not resolving the sheath, the electric field in the sheath is diminished by the ratio of $\lambda_s/\Delta x$. To compensate for the latter effect in the HPEM, we separately compute the conduction and displacement current to each location on the plasma-material boundary. With knowledge of the plasma density adjacent to the sheath (n_e) we can compute the expected rf sheath amplitude thickness using the Lieberman sheath model,[18]

$$\lambda_s = \frac{j_d}{\omega q n_e}, \quad \Delta x > \lambda_s \tag{1a}$$

$$\frac{\lambda_s}{\Delta x} = \left(\frac{j_{d0}}{\omega q n_e \Delta x} \right)^{1/2}, \tag{1b}$$

where j_d is the displacement current density and j_{d0} is its uncorrected value. If $\lambda_s < \Delta x$, then j_d is corrected. The revised value of j_d is then used to compute circuit parameters, among them the dc substrate bias. In the PCMCS, a similar procedure is followed to obtain the actual sheath thickness λ_s. This is an important consideration since the transit time of ions through the sheath relative to the duration of the rf cycle in part determines the shape of the ion energy distribution.[19–21] In the PCMCS the computational cell adjacent to a boundary is compressed to the actual sheath thickness so that transit time effects are more accurately represented.

III. PLASMA PROPERTIES WITH SUBWAFER DIELECTRICS

We will investigate an inductively coupled plasma (ICP) reactor having an rf bias applied to the substrate.[5–13] In this type of reactor, ionization is dominantly provided by the inductively coupled power as opposed to the substrate bias. Therefore, the consequences of the subwafer dielectrics are largely decoupled from plasma production. The thickness of the sheath, inversely proportional to the electron density, can also be independently varied (for a given rf bias) by varying the ICP power. This situation differs from conventional parallel plate capacitively coupled plasma reactors where power deposition (electron heating) is largely a result of sheath acceleration. Perturbation of the sheaths by subsurface dielectrics could therefore be expected to have an effect on ion production. RIE reactors will be addressed in a separate communication. The working gas for this study is argon. The electron impact cross sections and heavy particle collisions used in the model are discussed in Ref. 22.

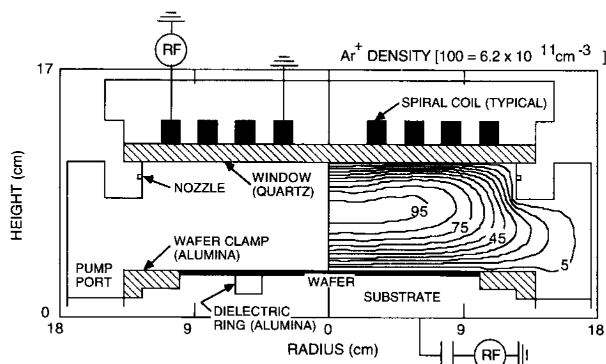

FIG. 1. Schematic of the inductively coupled plasma (ICP) reactor used in this study. The plasma is produced by a spiral coil placed on top of the dielectric window powered at 13.56 MHz. An rf bias, also at 13.56 MHz, is applied to the substrate. To investigate subwafer structures, a dielectric ring is placed under the wafer, as shown in the left panel. The time averaged ion density in the absence of the ring is shown in the right panel (Ar, 5 mTorr, 800 W, 100 V rf bias).

The ICP reactor is modeled after the LAM Research Inc. 9400 and 9600 series etching tools, and is schematically shown in Fig. 1.[11–13] The 13.56 MHz inductively coupled field is produced by a flat spiral coil (resolved as nested annuli in the model) set on top of a dielectric window. The wafer to window spacing is 7.5 cm. The 200 mm wafer sits on an rf biased substrate (100 V amplitude in this study). The subwafer dielectric we have investigated is an alumina ring flush to and embedded in the metal substrate as shown in the left panel of Fig. 1. The dielectric ring is 1.5 cm thick and 1.8 cm wide. The wafer is in electrical contact with the substrate and dielectric ring, and is assumed to be a lossless dielectric.

The rf cycle averaged ion density is shown in Fig. 1 for an ICP reactor (5 mTorr) without a subsurface dielectric. The ICP power is 800 W. The peak plasma density is 6.2×10^{11} cm^{-3}. The dc bias is -32 V. The ion density and plasma potential are fairly uniform across the wafer with a center to edge decrease of $\approx$10%. The rf cycle averaged ion density for an ICP reactor with a subwafer dielectric ring is shown in Fig. 2(a) in the vicinity of the dielectric. The plasma potential as a function of axial position at the center of the reactor and through the dielectric are shown in Fig. 2(b). There is clearly a perturbation in the ion density and plasma potential in the vicinity of the subsurface dielectric. Above the dielectric the sheath appears thinner and the cycle averaged sheath potential is smaller. As a consequence, the plasma is closer to the wafer above the dielectric on a cycle averaged basis. The

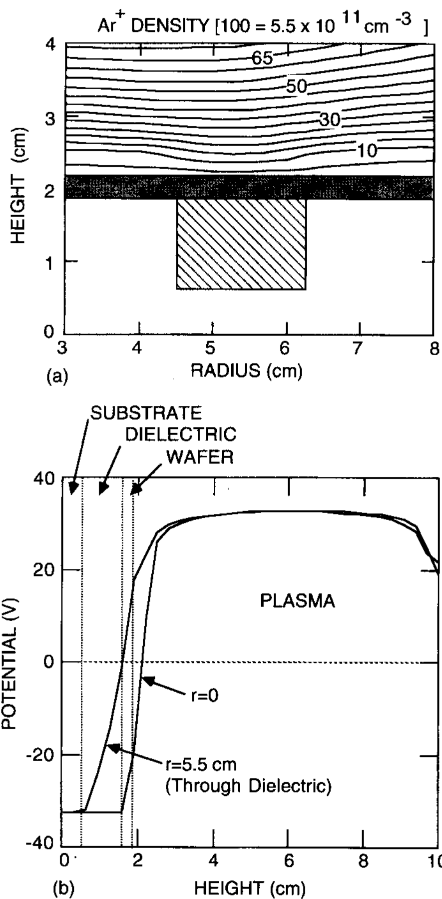

FIG. 2. Time averaged plasma properties for an ICP reactor with a subwafer dielectric ring. (a) Ar^+ density in the vicinity of the ring, (b) axial electric potential at the center of the plasma and at the radius of the dielectric ring.

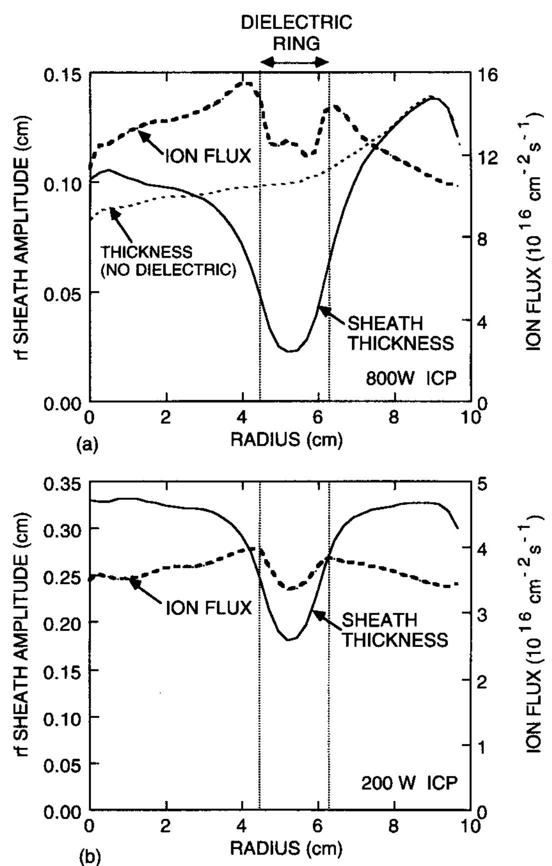

FIG. 3. Time averaged sheath thickness and ion flux to the wafer when operating with a dielectric ring. (a) 800 W ICP power, (b) 200 W ICP power. The sheath thickness is thinner above the dielectric. The effect is less severe at low ICP power when the sheath is thicker.

perturbation in plasma properties extends laterally beyond the subsurface dielectric by perhaps 1 cm.

In the absence of the subwafer dielectric, the plasma-sheath-wafer-substrate stack can be modeled as an equivalent circuit consisting of series resistors and capacitors. The series components are R_p(plasma)-C_s(sheath)-C_w(wafer)-V(voltage source). In the presence of the dielectric, an additional series capacitor C_d is placed between the wafer. and the voltage source. The equivalent circuit is then R_p-C_s-C_w-C_d-V. In this example, C_d is smaller than or commensurate to either C_w or C_s. Therefore, a large fraction of the applied voltage is dropped across C_d. As a consequence, the sheath voltage is smaller, which produces a thinner sheath.

One can also see the consequences of a thinner sheath (and lower sheath potential) above the wafer clamp in the right panel of Fig. 1. The time averaged ion density is closer to the wafer clamp than it is the wafer. The alumina wafer clamp is thick, and therefore has a small capacitance compared to the sheath or wafer. It therefore plays the same role as the subwafer dielectric with respect to voltage division and lowering the sheath potential in the plasma above it.

The time averaged ion flux and sheath thickness obtained from the HPEM are shown as a function of radius in Fig. 3(a) for the conditions of Figs. 1 and 2. The sheath thickness in the absence of the subwafer dielectric increases towards larger radius since the plasma density decreases. The sheath thickness with the subwafer dielectric has a local minimum above the dielectric which extends 1–2 cm beyond the dielectric The ion flux also has a small minimum above the dielectric, which is more localized to the dielectric. It should be noted, however, that the ion flux computed using the PCMCS has a smaller "dip" above the dielectric. The ion flux calculated in the HPEM does not take into account long mean free path effects, and hence should be considered a worst case.

The consequences of the subwafer dielectric depends on the ICP power since the plasma density scales nearly linearly with power deposition. The time averaged ion flux and sheath thickness are shown in Fig. 3(b) for an ICP power deposition of 200 W. The lower plasma density produces a thicker sheath which has a smaller capacitance. As a result, the additional series capacitance of the subsurface dielectric has a smaller perturbing effect compared to the high power case. The sheath thickness still has a minimum above the dielectric, but its relative depth is smaller. The ion flux also has a small minimum above the dielectric. However, the ion flux obtained from the PCMCS is nearly uniform.

On a time averaged basis, the sheath potential and thickness above the dielectric are reduced. However these quantities dynamically vary during the rf cycle. For example, a

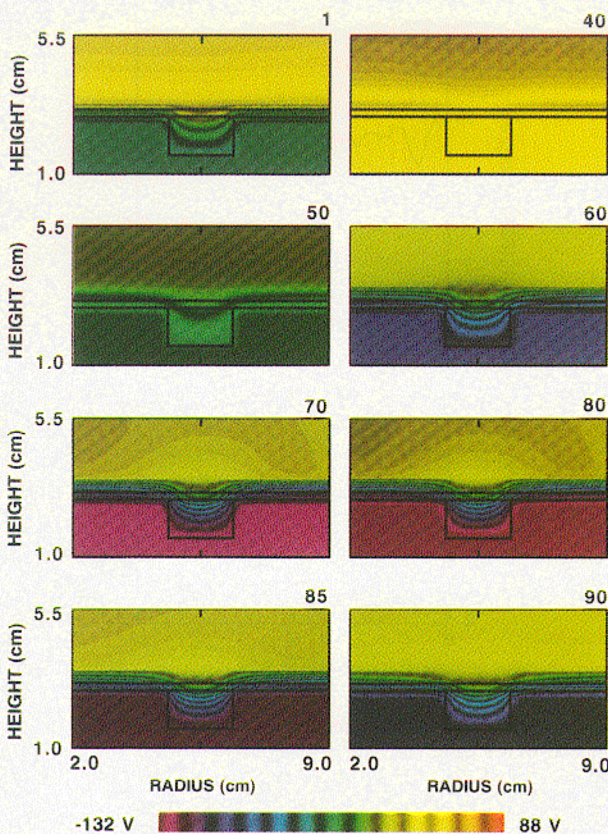

FIG. 4. Electric potential in the vicinity of the dielectric at various times during the rf cycle. The outline of the wafer and dielectric are shown. The numbers at the top right of each frame denote the time during the rf cycle (1–100). The dc bias is −32 V, the rf amplitude is V_0=100 V and the rf voltage is $V_0 \sin(\omega t)$ beginning with Frame 1. The potential in the plasma is perturbed to distances as far as 2 cm from the dielectric.

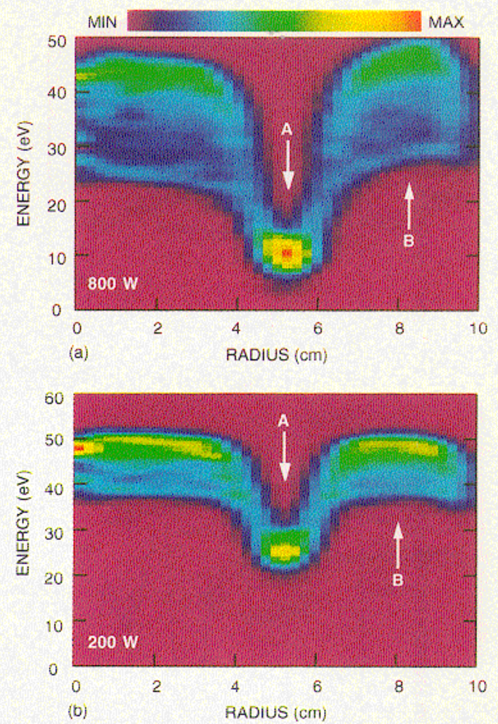

FIG. 5. Ion energy distributions striking the wafer as a function of radius for the (a) 800 W ICP case and (b) 200 W ICP cases. The IED is depressed in the vicinity of the dielectric due to the reduced sheath potential.

sequence of the electric potential at eight times during the rf cycle is shown in Fig. 4. The dc bias is −32 V. The applied rf potential is positive during the first half of the rf cycle (frames 1–50) and negative during the second half of the rf cycle (frames 51–100). During all portions of the rf cycle, the voltage drop across the subwafer dielectric reduces the sheath potential and produces a thinner sheath. During the anode portion of the cycle, the sheath potential is smaller, and so the differences in sheath potential above the subwafer dielectric compared to other locations is smaller. The effect is more severe during the cathode portion of the rf cycle when the sheath potential is larger. The largest perturbation in the plasma potential far from the dielectric occurs when the substrate is at its most negative voltage and increasing towards positive values. The perturbation in plasma potential extends more than 2 cm above the wafer and laterally beyond the dielectric. At this time, the sheath is collapsing as electrons begin moving towards the wafer. The substrate impedance at the radius of the dielectric is higher than adjacent regions. From a circuit standpoint, this reduces the current flowing to the wafer at the radii of the dielectric. The potential collapse is therefore slowed.

The ion energy distributions (IEDs) obtained from the PCMCS for Ar^+ striking the wafer as a function of radius are shown in Figs. 5 and 6 for the high and low power cases. The IEDs are shown as a function of radius in Fig. 5. The IEDs at the center of the dielectric and far away from the dielectric are shown in Fig. 6. Due to the thin sheath resulting from the large plasma density, the ions in the high power case have a short transit time across the sheath. The ions therefore experience nearly the instantaneous sheath potential as opposed to the time averaged sheath potential. As a result the IED has the characteristic two peak shape typically associated with conventional capacitively coupled RIE etching tools operating at low frequencies (100 kHz to a few MHz) or with light ions at 13.56 MHz.[19] Typically the sheath transit time for heavy ions is sufficiently long in reactors operating at 13.56 MHz and at low plasma density ($\leqslant 10^{10}$ cm^{-3}) that the IED has a single peak.[19,20]

Far from the subwafer dielectric, the IED in the high power case is uniform as a function of radius, but narrows slightly at large radius. This narrowing is a result of the lower plasma density at large radius which produces a thicker sheath, thereby lengthening the transit time. In the vicinity of the dielectric, the IED has a "dip" in energy. This decrease is a result of the reduced sheath potential above the dielectric, a consequence of the cited voltage division between the sheath, wafer, and dielectric. Note that the perturbation of the IED extends approximately 1 cm beyond the edge of the dielectric. The fact that the IED has a single peak in the vicinity of the dielectric is less a consequence of a long transit time than a small rf amplitude. The average angle of incidence of ions is shown in Fig. 7 as a function of

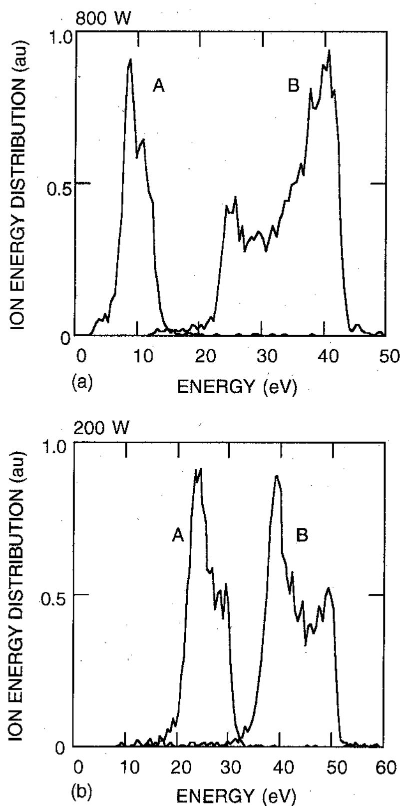

FIG. 6. Ion energy distributions striking the wafer at locations "A" and "B" denoted in Fig. 5(a) 800 W ICP case and (b) 200 W ICP case.

position on the wafer. Due to the thinner sheath and lower sheath voltage, the average angle of ions striking the wafer is larger above the dielectric. The average angle, approximately 7°, is commensurate to that seen in low pressure RIE tools having similar rf biases.[21]

The IED for the low power case, is less perturbed compared to the high power case. Recall that the sheath is thicker at low power due to the lower plasma density. The thicker sheath results in a longer ion transit time across the sheath, resulting in the ions residing in the sheath for proportionally more rf cycles. The end result is the IED has a narrower width about the time averaged sheath potential. The dc potential is also more negative. This has little to do with the presence of the dielectric but is rather a characteristic of ICP discharges. For a given rf bias amplitude, the dc bias is often observed to become more negative at lower ICP powers.[11,23,24] As with the high power case, the average energy of the ion flux is decreased in the vicinity of the subwafer dielectric. However the magnitude of the decease in ion energy is less. This is a result of the thicker sheath having a smaller capacitance and as a consequence the amount of voltage division with the subwafer dielectric is proportionally smaller.

The reduction in ion energy and flux above the dielectric may produce a reduction in etching rate at those locations for ion driven processes. For example, the outlines of gas distribution channels under the wafer (a "dielectric" with a unity relative permittivity) have been observed when etching SiO_2 using CF_4 gas mixtures. These observations were made in an

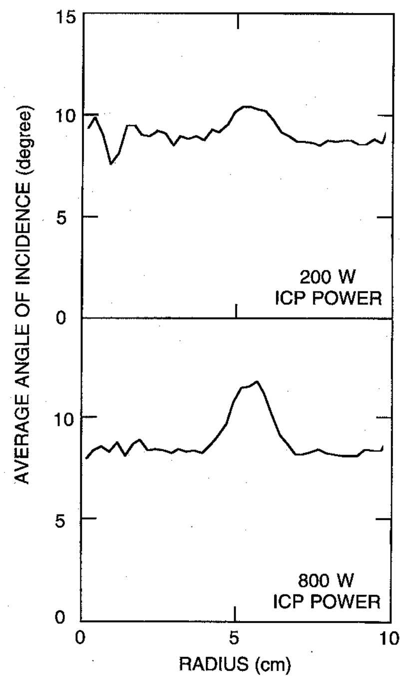

FIG. 7. Ion angular distribution to the wafer as a function of radius for the 200 and 800 W ICP case. The IAD is wider above the dielectric due to the reduced sheath potential.

ICP reactor having an electrostatic chuck.[25] The etch rate for this ion driven process was lower above the channels where the ion energies are expected to be lower.

IV. CONCLUDING REMARKS

The consequences of subwafer dielectrics in plasma etching tools have been computationally investigated. We found that dielectric structures positioned between the wafer and the driven electrode alter the local impedance (Ω cm^{-2}). If the capacitance of the dielectric is small compared to the wafer and sheath, voltage division will result in a significant fraction of the applied voltage to be dropped across the dielectric. As a result, less voltage is locally dropped across the sheath. This results in a thinning of the sheath and perturbation of the plasma. In ICP etching tools where ionization is largely decoupled from the applied rf bias, the perturbed sheath is manifested in a reduced current density (conduction and displacement) to the wafer above the dielectric. The ion energy distribution is also lowered in energy above the dielectric. These effects will be mitigated by highly conductive wafers which appear to be an equipotential plane, thereby shielding the plasma from nonuniform permittivities below the wafer.

ACKNOWLEDGMENTS

This work was supported by the National Science Foundation, Sandia National Laboratory/Sematech, Semiconductor Research Corporation and the University of Wisconsin ERC for Plasma Aided Manufacturing. The authors would like to thank Dr. Manoje Dalvie (IBM/Sematech) and Professor Claude Woods (University of Wisconsin) for discussions on the topic of this article.

[1] S. M. Rossnagel, in *Thin Film Processes II*, edited by J. L. Vossen and W. Kern (Academic, Boston, 1991), Chap. 1.
[2] M. Dalvie, M. Surrendra, G. S. Selwyn, and G. Guarnieri, Proceedings of the 41st National Symposium of the American Vacuum Society, Denver, CO, October 1994; paper MS-MoA6.
[3] G. S. Selwyn, Plasma Sources Sci. Technol. **3**, 340 (1994), and references therein.
[4] G. S. Selwyn, M. Dalvie, C. R. Guarnieri, and M. Surendra, Proceedings of the 41st National Symposium of the American Vacuum Society, Denver, Co, October 1994; paper MS-WeM5.
[5] J. Hopwood, Plasma Sources Sci. Technol. **1**, 109 (1992).
[6] Solid State Technol. **36**, 30 (1993).
[7] J. Keller, M. S. Barnes, and J. C. Forster, 42th Gaseous Electronics Conference, paper NA-5, Urbana, IL, 1990.
[8] J. H. Keller, J. C. Forster, and M. S. Barnes, J. Vac. Sci. Technol. A **11**, 2487 (1993).
[9] M. S. Barnes, J. C. Forster, and J. H. Keller, Appl. Phys. Lett. **62**, 2622 (1993).
[10] J. A. O'Neill, M. S. Barnes, and J. H. Keller, J. Appl. Phys. **73**, 1621 (1993).
[11] R. Patrick, R. Schoenborn, and H. Toda, J. Vac. Sci. Technol. A **11**, 1296 (1993).
[12] J. B. Carter, J. P. Holland, E. Peltzer, B. Richardson, E. Bogle, H. T. Nguyen, Y. Melaku, D. Gates, and M. Ben-Dor, J. Vac. Sci. Technol. B **11**, 1301 (1993).
[13] Y. Ra, S. G. Bradley, and C.-H. Chen, J. Vac. Sci. Technol. A **12**, 1328 (1994).
[14] P. L. G. Ventzek, R. J. Hoekstra, T. J. Sommerer, and M. J. Kushner, Appl. Phys. Lett. **63**, 605 (1993).
[15] P. L. G. Ventzek, R. J. Hoekstra, and M. J. Kushner, J. Vac. Sci. Technol. B **12**, 461 (1994).
[16] P. L. G. Ventzek, M. J. Grapperhaus, and M. J. Kushner, J. Vac. Sci. Technol. B **12**, 3118 (1994).
[17] M. J. Hartig and M. J. Kushner, Appl. Phys. Lett. **62**, 1594 (1993).
[18] M. A. Lieberman, Trans. Plasma Sci. **17**, 338 (1989).
[19] K. Kohler, D. E. Horne, and J. W. Coburn, J. Appl. Phys. **58**, 3350 (1985).
[20] A. Manenschijn, G. C. A. M. Janssen, E. van der Drift, and S. Radelaar, J. Appl. Phys. **69**, 1253 (1991).
[21] J. Liu, G. L. Huppert, and H. H. Sawin, J. Appl. Phys. **68**, 3916 (1990).
[22] T. J. Sommerer and M. J. Kushner, J. Appl. Phys. **71**, 1654 (1992).
[23] T. Fukasawa, T. Nouda, A. Nakamura, H. Shindo, and Y. Horiike, Jpn. J. Appl. Phys. **32**, 6076 (1993).
[24] Y. Ra and C.-H. Chen, J. Vac. Sci. Technol. A **11**, 2911 (1993).
[25] C. Woods, University of Wisconsin Engineering Research Center for Plasma Aided Manufacturing (private communication, 1994).